# Syntheses and structural characterization of metal complexes of 4-(naphthalen-1-yl)-1-(quinolin-2-yl)methylene)thiosemicarbazide: their *in-vitro* screening studies for antitubercular activity

Pooja Lokesh Hegde, Krishna Naik, Satish S. Bhat, Sabiha A. Shaikh, Ray J. Butcher, Naveen S., N. K. Lokanath & Vidyanand K. Revankar

View supplementary material

Published online: 29 Nov 2021.

Submit your article to this journal

Article views: 23

View related articles

View Crossmark data

Taylor & Francis
Taylor & Francis Group

Check for updates

# Syntheses and structural characterization of metal complexes of 4-(naphthalen-1-yl)-1-(quinolin-2-yl)methylene)thiosemicarbazide: their *in-vitro* screening studies for antitubercular activity

Pooja Lokesh Hegde[a], Krishna Naik[b], Satish S. Bhat[a] (iD), Sabiha A. Shaikh[a], Ray J. Butcher[c], Naveen S.[d], N. K. Lokanath[e] and Vidyanand K. Revankar[a]

[a]P. G. Department of Studies in Chemistry, Karnatak University, Dharwad, India; [b]Department of Chemistry, Karnataka Science College, Dharwad, India; [c]Department of Chemistry, Howard University, Washington, DC, USA; [d]Department of Physics, School of Engineering & Technology, Jain (Deemed-to-be University), Bangalore, India; [e]Department of Studies in Physics, University of Mysore, Manasagangotri, Mysuru, Karnataka, India

## ABSTRACT

The ligand 4-(naphthalen-1-yl)-1-((quinolin-2-yl)methylene)thiose-micarbazide (**HL**) and its cobalt(III), nickel(II) and copper(II) complexes of type $[Co^{III}L_2]Cl$ (**1**), $[Ni^{II}L_2]$ (**2**), $[Cu^{II}LCl]$ (**3**) were synthesized and structurally characterized by various spectral techniques. The structure of **2** was confirmed through single-crystal X-ray structure determination. Complex **2** crystallized in the triclinic system with the *P*-1 space group. **HL** acts as tridentate chelate with N,N,S-donor sites. The spectrochemical analysis of all the complexes showed that, in the case of **1** and **2**, the metal-to-**L** ratio is 1:2, while in the case of **3**, the copper-to-ligand ratio is 1:1. The antitubercular studies of the complexes were explored *in vitro* against the *Mycobacterium* strain, *M. H37Rv*. Complex **3** has better activity compared to the standard drug pyrazinamide. Cytotoxicity studies were carried out on human embryonic kidney cell lines (HEK293). Inhibition of tuberculosis bacteria has increased upon complexation compared to the free ligand.

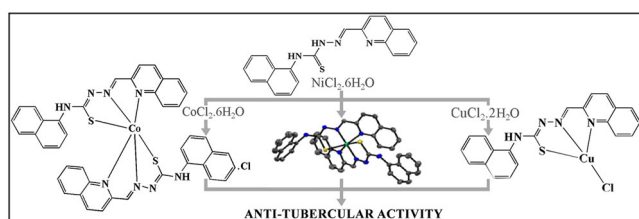**CONTACT** Vidyanand K. Revankar ✉ vkrevankar@rediffmail.com P. G. Department of Studies in Chemistry, Karnatak University, Dharwad 580003, India.

Supplemental data for this article is available online at https://doi.org/10.1080/00958972.2021.2007892.

## 1. Introduction

According to the World Health Organization (WHO), tuberculosis (TB), caused by the bacillus *Mycobacterium tuberculosis* (Mtb), is one of the top ten reasons for death across the globe. In 2019, 10 million TB cases were reported worldwide, of which more than 1.2 million cases were fatal [1]. Certain TB strains have developed resistance to the two most potent TB drugs, isoniazid and rifampicin, leading to multi-drug resistant tuberculosis (MDR-TB) [2]. Similarly, some TB strains have also developed resistance to fluoroquinolone and one of the second-line drugs (amikacin, kanamycin, or capreomycin) in addition to MDR-TB leading to extensively drug-resistant tuberculosis (XDR-TB) [3]. This makes treating MDR and XDR-TB expensive and complicated, posing a serious threat to humanity [4–7]. Therefore, many research groups across the world are working diligently to develop an effective antitubercular treatment [8,9]. In these studies, molecules derived from the thiosemicarbazide core have exhibited promising activity as anti-TB agents (Figure 1) [10–12]. The mechanism of action for thiosemicarbazone is poorly known. From this chemical class, thiacetazone (one of the oldest and cheapest second-line drugs available) has given some elusive results on the mechanism of action for the anti-TB drug. It has been shown that thiacetazone affects mycolic acid synthesis in TB bacteria [13]. In many cases complexation of the ligand having a thiosemicarbazone scaffold has shown improved activity [14]. Thiosemicarbazide and its derivatives have a wide range of biological applications. To name a few, these are used to combat HIV-TB co-infection [15], tumors [16], malaria [17], and fungal infections [18].

Recently, molecules containing a quinoline core are attracting interest in the field of TB due to the clinical use of some quinoline derivatives like ciprofloxacin, mefloquine, bedaquiline (also called TMC-207) as anti-TB drugs (Figure 1) [19,20]. Bedaquiline has entered phase-III clinical trials and was found effective against the highly resistant form of tuberculosis strain [21]. A mechanistic study of bedaquiline revealed that it inhibits the proton pump of *M. tuberculosis* ATP synthase [22]. Quinolines and their derivatives also have other pharmaceutical applications as anticancer [23], antimalarial [24], antimicrobial [25], and anti-inflammatory [26] agents.

Liu *et al.* reported a novel ligand containing both a thiosemicarbazide and quinoline moiety and its copper(II) complex and they have studied its interaction with calf-thymus DNA by an intercalation mechanism [27]. Adsule *et al.* explored the antiproliferative activity of novel copper(II) complexes having both a thiosemicarbazide and quinoline scaffold as proteasome inhibitors in human prostate cancer cells [28].

The above literature laid a path for us to design a ligand and its metal complexes having thiosemicarbazide and quinoline-base structures as parent molecules (Figure 2), and to explore their pharmaceutical importance. Herein, we report the synthesis and structural characterization of novel ligand 4-(naphthalen-1-yl)-1-((quinolin-2-yl)methylene)thiosemicarbazide (**HL**) and its complexes [Co$^{III}$L$_2$]Cl (**1**), [Ni$^{II}$L$_2$] (**2**), and [Cu$^{II}$LCl] (**3**). The molecular structure of **2** was established using single-crystal X-ray structure determination. The anti-TB activity and cytotoxicity of the synthesized compounds were investigated.
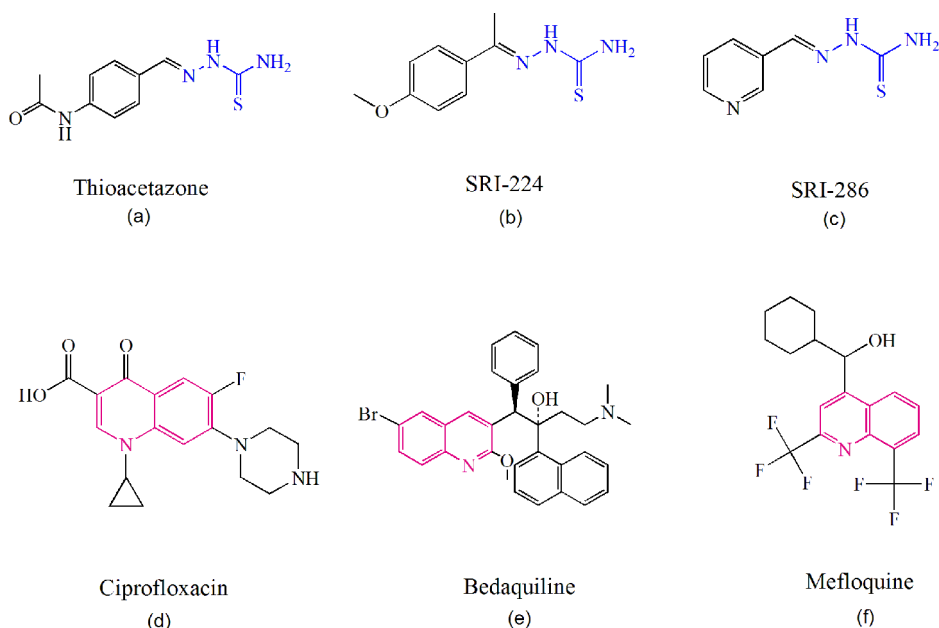
**Figure 1.** Molecular structures of reported anti-TB drugs derived from thiosemicarbazide (a–c) and quinoline (d–f) scaffold.
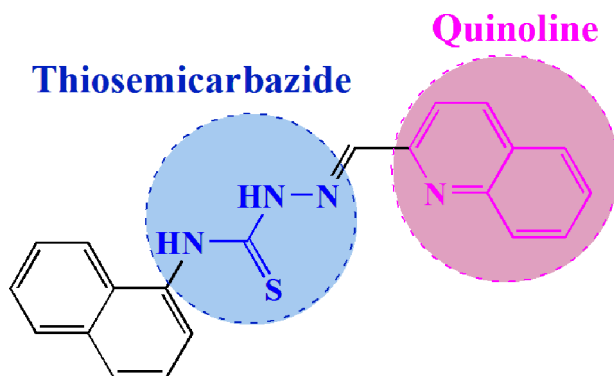


**Figure 2.** The design strategy for **HL** synthesis.

## 2. Experimental

### 2.1. Chemistry

All chemicals used for the syntheses were purchased from SD Fine Chemicals Ltd. (India) and used without purification. FT-IR was recorded on the KBr pellet from 4000 to 400 cm$^{-1}$ on a Nicolet-6700. $^1$H and $^{13}$C NMR spectra was recorded on a JEOL ECZ 400 MHz spectrometer in deuterated dimethylsulphoxide (DMSO-d$_6$) and values are expressed in δ (in ppm). FLASH EA 1112 model by Thermo Finnigan and Perkin Elmer-2400 series 2 elemental analyzer were used for elemental analyses. Mass spectra of ligand and complexes were recorded on Shimadzu QP210S and Waters SYNAPTG2, respectively. The molar conductivity measurements were made on a Systronics

conductivity TDS meter 308. TGA-DTA analyses were carried out on the SDT Q600 V20.9 build-20. UV-vis spectra of compounds were recorded at room temperature on the JASCO V-670 spectrophotometer. A VARIAN E-112 X-band ESR spectrometer was used for Electron Spin Resonance (ESR) study.

### 2.1.1. Synthesis of HL

One of the reactants, 4-(naphthalene-1-yl)thiosemicarbazide, was prepared as in literature [29]. A methanolic solution of quinoline-2-carboxaldehyde (0.217 g, 1.38 mM) was added to a methanolic solution of 4-(naphthalene-1-yl)thiosemicarbazide (0.300 g, 1.38 mM) and the mixture was stirred for 8 h at room temperature (RT). The precipitated compound **HL** was filtered and recrystallized in ethanol. Yield: 0.449 g (91%). FT-IR (KBr), $v$ (cm$^{-1}$): 3290 (N–H), 3050, 1620, 1591 (C=N), 1555 (–N-C=S), 1500 (C=C),1469, 1417,1333 (–N–C=S), 1269, 1184, 1144, 1090, 1058 (–N–C=S), 974, 951, 936, 907 (C=S), 828, 804, 777, 745, 639, 611, 560, 528, 474, 449; $^1$H NMR (DMSO-d$_6$, 399.87 MHz), $\delta$ (ppm): 12.29 (s, 1H), 10.67 (s, 1H), 8.61(d, 1H), 8.35 (s, 1H), 8.32 (d, 1H), 7.93 (m, 5H), 7.74 (dd, 1H), 7.53 (m, 5H); $^{13}$C NMR (DMSO-d$_6$, 100.53 MHz), $\delta$ (ppm): 178.86, 154.41, 147.85, 143.46, 136.83, 136.11, 134.24, 131.09, 130.55, 129.31, 128.58, 128.48, 128.42, 127.78, 127.73, 127.13, 126.75, 126.67, 126.05, 123.94, 119.03; MS (EI) m/z: calcd. for $C_{21}H_{16}N_4S^-$ 356.11; found- 356 [M$^+$]. Anal. calc. for $C_{21}H_{16}N_4S$ (%): C, 70.76; H, 4.52; N, 15.72. Found: C, 70.53; H, 4.55; N, 15.42.

### 2.1.2. Synthesis of [Co$^{III}$L$_2$]Cl (1)

A methanolic solution of cobalt(II) chloride hexahydrate (0.050 g, 0.21 mM) was added to the hot methanolic solution of **HL** (0.150 g, 0.42 mM) and refluxed for 8 h. The clear solution obtained was cooled, filtered and kept for evaporation at RT. A brown precipitate was obtained after a few days which was then recrystallized in ethanol. Yield: 0.132 g (78%). FT-IR (KBr), $v$ (cm$^{-1}$): 3290 (N–H), 3051, 1626, 1595 (C=N), 1549 (–N–C=S), 1513 (C=C), 1491, 1468, 1421, 1339 (–N–C=S), 1263, 1209, 1114, 1078 (–N–C=S), 1015, 994, 938, 871, 769, 673 (C–S), 597, 491; $^1$H NMR (DMSO-d$_6$, 399.87 MHz), $\delta$ (ppm): 11.03 (s, 2H), 9.11 (s, 2H), 8.58 (d, 2H), 8.01(t, 6H), 7.93 (d, 2H), 7.86 (d, 2H), 7.79 (t, 2H), 7.66 (t, 2H), 7.58 (d, 2H), 7.49 (t, 4H), 7.41 (d, 2H), 7.27 (d, 2H); $^{13}$C NMR (DMSO-d$_6$, 100.53 MHz), $\delta$ (ppm): 159.75, 153.34, 147.94, 141.87, 135.28, 134.35, 133.93, 130.87, 129.28, 129.09, 128.85, 128.15, 127.04, 126.97, 126.15, 124.80, 124.65, 123.41, 123.21, 123.35, 66.89; ESI-MS (positive mode) m/z: ([CoL$_2$]$^+$) 769.02. Anal. calc. for $C_{42}H_{30}ClCoN_8S_2$ (%): C, 62.64; H, 3.76; N, 13.92. Found: C, 62.43; H, 3.68; N, 13.53.

### 2.1.3. Synthesis of [Ni$^{II}$L$_2$] (2)

The methanolic solution of nickel(II) chloride hexahydrate (0.050 g, 0.21 mM) was added to the hot methanolic solution of **HL** (0.150 g, 0.42 mM) and refluxed for 8 h. The clear solution obtained was cooled, filtered and kept for evaporation at RT. The brown precipitate obtained was dissolved in dimethylformamide (DMF) and kept for evaporation at RT. After several days, single crystals suitable for X-ray crystallography were obtained. Yield: 0.130 g (80%). FT-IR (KBr), $v$ (cm$^{-1}$): 3296 (N–H), 2963, 2785, 1618, 1596, 1580 (C=N), 1519 (–N–C=S), 1500 (C=C), 1465, 1434, 1390, 1337, 1315

(–N–C = S), 1258, 1191, 1134, 1112, 1077, 1042 (–N–C = S), 1017, 989, 886, 823, 768, 744, 675 (C–S), 602, 562, 487; ESI-MS (positive mode) m/z: ([NiL$_2$–H]$^+$) 769.02. Anal. calc. for C$_{42}$H$_{30}$N$_8$NiS$_2$ (%): C, 65.55; H, 3.93; N, 14.56. Found: C, 65.63; H, 3.81; N, 14.33.

### 2.1.4. Synthesis of [Cu$^{II}$LCl] (3)

To the methanolic solution of **HL** (0.100 g, 0.28 mM), a methanolic solution of copper(II) chloride dihydrate (0.048 g, 0.28 mM) was added and stirred for 10 h at RT. The precipitate obtained was filtered, washed with small amount of cold methanol and air dried. Yield: 0.110 g (86%). FT-IR (KBr), $v$ (cm$^{-1}$): 3335 (N–H), 3050, 1591 (C = N), 1525 (–N–C = S), 1504 (C = C), 1476, 1452, 1431, 1372, 1345 (–N–C = S), 1282, 1243, 1210, 1143, 1117, 1037 (–N–C = S), 941, 899, 799, 771, 748, 674 (C–S), 622, 556, 521, 485; ESI-MS (m/z, positive mode): ([CuL–Cl–H]$^+$) 417.95. Anal. calc. for C$_{21}$H$_{15}$ClCuN$_4$S (%): C, 55.50; H, 3.33; N, 12.33. Found: C, 55.65; H, 3.75; N, 12.36.

## 2.2. X-Ray crystallography

Single-crystal X-ray diffraction data of **2** was obtained at 296 K on a Bruker *SMART* X2S benchtop CCD area detector diffractometer using a graphite monochromated Mo-Kα radiation source. The structure was solved on Olex2-1.2 [30] with the ShelXT [31] structure solution program using Intrinsic Phasing and refined with XL refinement package [31] using Least Squares Minimization. All non-hydrogen atoms were refined anisotropically. Badly-disordered solvent molecules (DMF) could not be resolved and were removed using the SQUEEZE routine from Platon [32]. These solvent molecules were located in special positions with a volume of 417 Å$^3$ and SQUEEZE indicated that this corresponds to 84 electrons [2 DMF molecules (DMF, C$_3$H$_7$NO, 40 electrons)]. Mercury-4.1.3 package was used to generate molecular graphics. CCDC 1972174 contains the supplementary crystallographic data for this article which is available at https://www.ccdc.cam.ac.uk/structures/.

## 2.3. In-vitro antitubercular activity

The antitubercular activity of the compounds was evaluated against the *M. tuberculosis H37Rv* strain using Microplate Alamar Blue Assay (MABA) [33]. In brief, 200 μL of sterile deionized water was added to all outer perimeter wells of a sterile 96-well plate to minimize the evaporation of the medium in the test wells during incubation. The 96-well plate received 100 μL of the Middlebrook 7H9 broth and serial dilution of compounds was made directly on the plate. The final drug concentrations tested were 100–0.2 μg/mL. Plates were covered and sealed with parafilm and incubated at 37 °C for five days. After this time, 25 μL of freshly prepared 1:1 mixture of Almar Blue reagent and 10% Tween 80 was added to the plate and incubated for 24 h. The blue color in the well was interpreted as no bacterial growth, and the pink color was scored as growth. The minimum inhibitory concentration (MIC) was defined as the lowest drug concentration which prevented the color change from blue to pink.
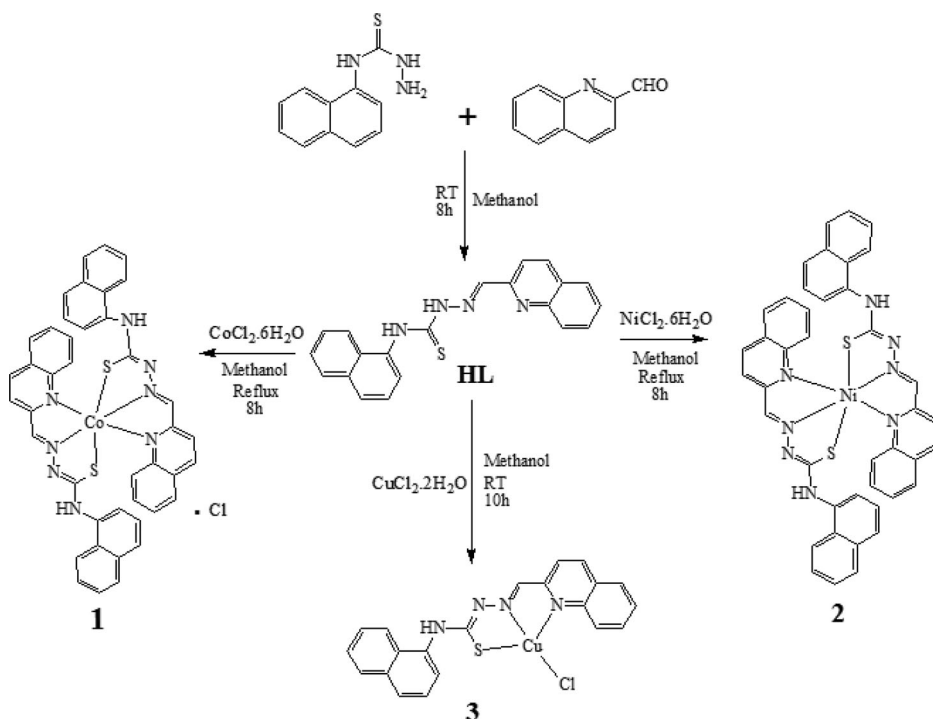
**Scheme 1.** Synthetic route for **HL** and its metal complexes.

## 2.4. Cytotoxicity

Cytotoxicity studies were carried out on the human embryonic kidney cell line, HEK293, by MTT assay. The cells were seeded at a density of approximately $5 \times 10^3$ cells/well in a 96-well flat-bottom microplate and maintained at 37 °C in 95% humidity and 5% $CO_2$ overnight. The cells were treated with different concentrations (500, 250, 125, 62.5, 31.25, and 15.625 µg/mL) of the compounds and incubated for another 48 h. The cells in the well were washed twice with phosphate buffer solution. 20 µL of the MTT staining solution (5 mg/mL in phosphate buffer solution) was added to each well and the plate was incubated at 37 °C. After 4 h, 100 µL of DMSO was added to each well to dissolve the formazan crystals, and absorbance was recorded at 570 nm using a microplate reader [34].

## 3. Results and discussion

### 3.1. Synthesis and characterization

**HL** was synthesized by condensation of 4-(naphthalen-1-yl)thiosemicarbazide and 2-quinolinecarboxaldehyde (Scheme 1). Metal complexes were synthesized by reacting **HL** and metal salts with an appropriate mole ratio (Scheme 1). The synthesized complexes were characterized by FT-IR, ESI-MS, $^1$H, and $^{13}$C NMR, elemental analyses, UV–vis spectroscopy, and thermogravimetric analysis. The structure of **2** was determined by single-crystal X-ray crystallography.

FT-IR spectra of the ligand showed a band at 907 cm$^{-1}$ corresponding to $\nu(C=S)$. Upon complexation, this band disappeared and a new band appeared at 673, 675,
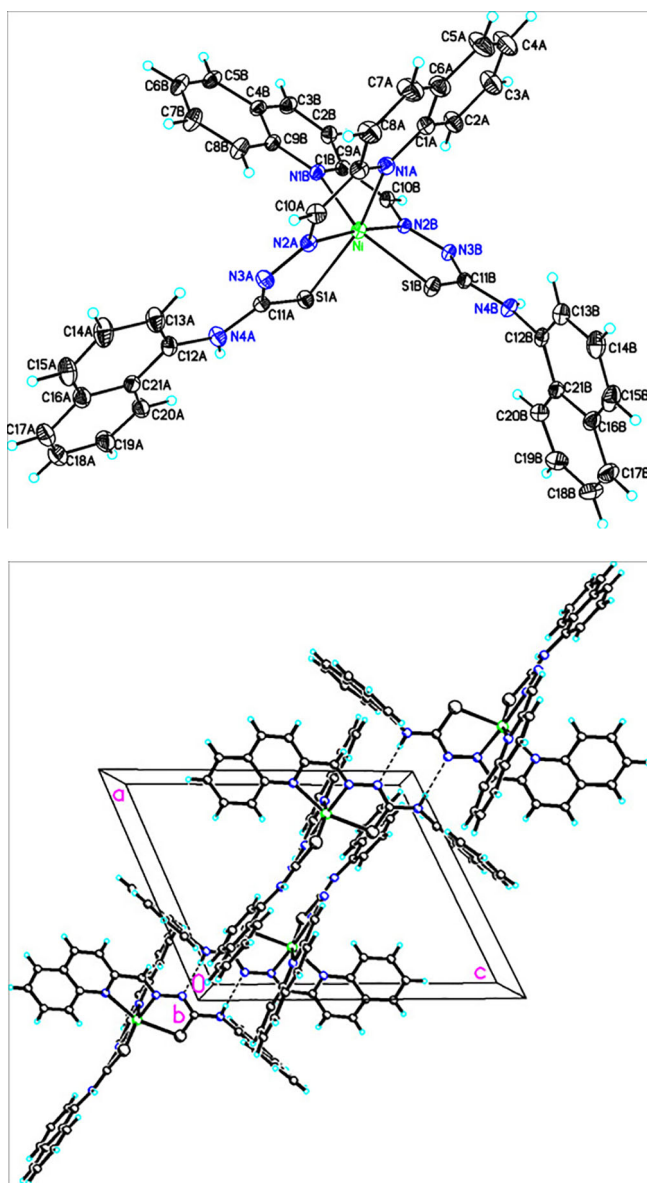
**Figure 3.** (a) ORTEP diagram of **2**. Hydrogen bonds are omitted for clarity. (b) Packing diagram of **2** showing strong intermolecular hydrogen bonding (2.283 Å).

and 674 cm$^{-1}$ for **1**, **2** and **3**, respectively, corresponding to $\nu$(C–S). This indicated the participation of thioamide sulfur in coordination [29, 35].

ESI-MS of the complexes in the positive mode were analyzed. Values corresponded to the proposed structure of the complexes (given in the Experimental section). ESI-MS of **1** indicated the *in situ* oxidation of Co(II)–Co(III) after complexation [36].

Proton and carbon NMR spectra of **HL** and **1** were recorded. NMR supported the diamagnetic nature of **1**, as expected for the low spin octahedral Co(III) complex [36,37]. In $^1$H NMR spectrum of **HL**, phenyl –NH and hydrazone –NH peaks were

**Table 1.** Selected crystallographic data for **2**.

| Empirical formula | $C_{42}H_{30}N_8NiS_2$ |
| --- | --- |
| Formula weight | 769.57 |
| Crystal system | Triclinic |
| Space group | $P-1$ |
| Temperature (K) | 296(2) |
| Unit cell dimensions: | $a = 12.1764(3)$ Å, $\alpha = 95.2750(10)°$ |
| | $b = 13.5808(3)$ Å, $\beta = 111.3480(10)°$ |
| | $c = 14.5921(4)$ Å, $\gamma = 109.9500(10)°$ |
| Volume (Å$^3$) | 2047.20(9) |
| $Z$ | 2 |
| Density (calculated) | 1.248 Mg/m$^3$ |
| Absorption coefficient | 0.615 mm$^{-1}$ |
| F(000) | 796 |
| Theta range for data collection | 1.646–23.898° |
| Index ranges | $^-13 \leq h \leq 13$, $-15 \leq k \leq 15$, $-15 \leq l \leq 16$ |
| Reflections collected | 23207 |
| Independent reflections | 6333 [R(int) = 0.0362] |
| Completeness to theta = 23.898° | 99.6% |
| Absorption correction | None |
| Refinement method | Full-matrix least-squares on F$^2$ |
| Data / restraints / parameters | 6333/0/486 |
| Goodness-of-fit on F$^2$ | 1.039 |
| Final R indices [I > 2sigma(I)] | R1 = 0.0328, wR2 = 0.0766 |
| R indices (all data) | R1 = 0.0466, wR2 = 0.0823 |
| Largest diff. peak and hole | 0.213 and −0.199 e.Å$^{-3}$ |

observed at 12.29 and 10.67 ppm, respectively [38] which was further confirmed by the D$_2$O exchange experiment. In the NMR spectrum of **1**, the phenyl –NH peak suffered an upfield shift at 11.03 ppm and the disappearance of the hydrazone –NH peak indicated the deprotonation during complexation. Azomethine proton of **HL** at 8.35 ppm underwent a downfield shift in **1** and was resonated at $\delta = 9.11$ ppm. In the $^{13}$C NMR spectrum of **HL** thioamide carbon and azomethine carbon peaks were observed at 178.8 and 154.4 ppm, respectively. In **1**, thioamide carbon has suffered an upfield shift at $\delta = 66.8$ ppm and azomethine carbon has shifted downfield at 159.7 ppm. These observations confirmed the participation of sulfur and nitrogen in complexation [39].

Molar conductance of all the complexes was measured at room temperature in DMF with 10$^{-3}$ M concentration. Conductance value 76.16 ohm$^{-1}$cm$^2$mol$^{-1}$ for **1** showed the 1:1 electrolytic nature of the complex. Complexes **2** and **3** were non-electrolytes with conductance value of 26.30 ohm$^{-1}$cm$^2$mol$^{-1}$ and 30.99 ohm$^{-1}$cm$^2$mol$^{-1}$, respectively [40].

Thermogravimetric analysis of **1** exhibited ligand degradation and chloride elimination above 200 °C which resulted in an exothermic peak around 220 °C in DTA [41]. In **3**, above 213.35 °C a weight loss of 36.77% was observed corresponding to the loss of part of ligand moiety along with the coordinated chloride as HCl which was observed as an exothermic peak in DTA.

### 3.1.1. Crystal structure
Single crystals of **2** were grown by slow evaporation of the complex in DMF at room temperature. Complex **2** crystallized in the triclinic system with the *P*-1 space group. An ORTEP representation of **2** with an atom numbering scheme is shown in Figure 3(a). A summary of the crystallographic parameters is compiled in Table 1. Important bond lengths and angles are given in Table 2. The geometry around the nickel center

**Table 2.** Selected bond lengths (Å) and angles (°) for **2**.

| Selected bond lengths | | | |
|---|---|---|---|
| Bond | Length (Å) | Bond | Length (Å) |
| Ni–N(1A) | 2.2016(18) | Ni–N(1B) | 2.2084(17) |
| Ni–N(2A) | 2.0068(18) | Ni–N(2B) | 2.0128(17) |
| Ni–S(1A) | 2.4097(6) | Ni–S(1B) | 2.3951(6) |
| Selected bond angles | | | |
| Bond | Angle (°) | Bond | Angle (°) |
| N(2A)–Ni–N(2B) | 174.23(7) | N(1A)–Ni–S(1B) | 89.29(5) |
| N(2A)–Ni–N(1A) | 77.87(7) | N(1B)–Ni–S(1B) | 158.08(5) |
| N(2B)–Ni–N(1A) | 107.29(7) | N(2A)–Ni–S(1A) | 80.39(5) |
| N(2A)–Ni–N(1B) | 104.38(7) | N(2B)–Ni–S(1A) | 94.57(5) |
| N(2B)–Ni–N(1B) | 78.41(7) | N(1A)–Ni–S(1A) | 158.05(5) |
| N(1A)–Ni–N(1B) | 91.23(6) | N(1B)–Ni–S(1A) | 91.26(5) |
| N(2A)–Ni–S(1B) | 97.16(5) | S(1B)–Ni–S(1A) | 96.39(2) |
| N(2B)–Ni–S(1B) | 80.51(5) | | |

in the complex had a distorted octahedral geometry and the two deprotonated $L^-$ moieties were arranged perpendicular to each other. The average Ni-S and Ni-N bond distances were 2.4024(6) and 2.1074(17) Đ, respectively, which were similar to the Ni-$N_2S$ type of complexes reported in the literature [42,43]. The packing diagram showed a strong intermolecular hydrogen bonding *via* N(4B)-H(4NB)…N(3B) between neighboring complex molecules (Figure 3(b)).

### 3.1.2. Electronic spectral studies
Electronic spectra of **HL** showed two bands at 342 nm and 357 nm corresponding to transition in the conjugated π-π-p-π electron system [37]. Upon complexation, these bands suffered a shift of around 310–320 nm (Figure 4) [44,45]. Bands observed at 415 nm in **1**, 404 nm in **2** and 455 nm in **3** were due to ligand-to-metal charge-transfer (LMCT) transition [46]. A weak band at 682 and 837 in **1** and **2,** respectively, indicated the d-d transition. The stability of the complexes was studied in DMF ($10^{-5}$ M). UV–vis spectra were recorded once immediately after dissolution, then after 4 h, 8 h and 24 h of dissolution, and no major changes were observed in the spectra (Figures S18–S20).

### 3.1.3. EPR spectral studies
Copper(II) complex **3** exhibited an axial EPR spectrum (Figure S18). The calculation showed the result, $g_{||}(2.1750) > g_{\perp}(2.0407) > g_e$ (=2.0023). This indicated the square planar geometry of **3** with an unpaired electron predominantly in $d_{x2-y2}$ orbital [47,48]. The exchange interaction term (G) was found to be greater than 4 ($G = 4.497$). This suggested that exchange interaction was not operative in **3** [49]. Also, the value of $g_{||}$ being less than 2.3 pointed out the considerable metal-to-ligand covalent character in the complex [50,51].

### 3.2. M. tuberculosis H37Rv inhibition

All the synthesized compounds were tested for antitubercular activity against the Mtb *H37Rv* strain using MABA [33]. The anti-TB activities of **1** and **2** were higher when compared to the free ligand **HL** (Table 3). The inhibition activity of **3** improved
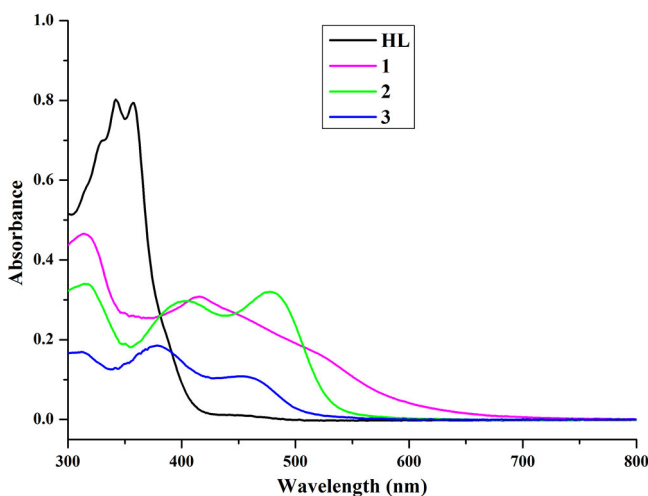
**Figure 4.** UV–vis data of ligand and its complexes in DMF with $10^{-5}$ M concentration.

**Table 3.** Inhibition of *M. tuberculosis* H37Rv by ligand HL and its complexes **1-3** and their cytotoxicity studies against human embryonic kidney (HEK293) cell lines. Selectivity index (SI) values are tabulated.

| Compounds | Antitubercular activity MIC (µM) | Cytotoxicity IC$_{50}$ (µM) | Selectivity Index (SI) |
|---|---|---|---|
| **HL** | 280.55 | 215.91 | 0.76 |
| **1** | 129.90 | 173.61 | 1.33 |
| **2** | 129.94 | 235.32 | 1.81 |
| **3** | 13.75 | 217.52 | 15.82 |
| Pyrazinamide | 25.38 | | |
| Streptomycin | 10.74 | | |
| Ciprofloxacin | 9.43 | | |

significantly with a MIC value of 13.75 µM. This was better than the standard drug pyrazinamide (25.38 µM) and comparable to streptomycin and ciprofloxacin. Such increased activity of the metal chelates could be explained based on Tweedy's chelation theory [52]. Chelation can increase lipophilicity, which in turn helps in the permeability of the moiety through the cell membrane of the target making it easier for the metal complexes to disturb the cell metabolism and thus restrict further growth of the organisms [53].

## 3.3. Cytotoxicity studies

The synthesized compounds were examined for their toxicity on human embryonic kidney cell lines (HEK293) after incubating for 48 h with concentrations ranging from 500 µg/mL to 15.625 µg/mlL. IC$_{50}$ values of all the complexes were higher than their respective MIC values for *M. H37Rv* inhibition (Table 3). Complexes **1** and **2** showed around one-fold higher IC$_{50}$ values when compared to MIC whereas copper complex **3** showed an almost fifteen-fold increase in IC$_{50}$ value (217.52 µM) when compared to the MIC value for TB bacillus (13.75 µM). This suggests that **3** shows promising antitubercular activity.

Selectivity index (SI) was calculated by dividing the compound's $IC_{50}$ value by its MIC value [54]. **HL** has SI < 1 and **1** and **2** showed SI > 1. For **3** SI value was found to be 15.82 (Table 3). Theoretically, if the SI value of a compound is more than 10, it is said to be effective and safe during *in vivo* treatment of TB infection [55]. This indicated that **3** has the potential to be an effective compound in TB treatment.

## 4. Conclusion

In this study, cobalt(III), nickel(II) and copper(II) complexes of the novel ligand 4-(naphthalen-1-yl)-1-((quinolin-2-yl)methylene)thiosemicarbazide were synthesized and characterized. The molecular structure of **2** was confirmed by single-crystal X-ray diffraction. Complex **1** has undergone *in situ* oxidation from Co(II) to Co(III). Among the synthesized compounds, **3** has shown high inhibition of *M. H37Rv*. The cytotoxicity value for **1** and **2** is higher by one-fold whereas the cytotoxicity of **3** is fifteen times higher than the corresponding MIC values. Complexation of the free ligand has increased the inhibition rate of *M. H37Rv*, copper complex being the better inhibitor.

## Acknowledgment

## Disclosure statement

## ORCID

Satish S. Bhat 🔟 http://orcid.org/0000-0002-3250-9966

## References

[1]   Global Tuberculosis Report 2020, World Health Organization, Geneva (2020). https://www. who.int/teams/global-tuberculosis-programme/data.
[2]   R.F. Jacobs. *Semin. Pediatr. Infect. Dis.*, **7**, 170 (1996).
[3]   P. LoBue. *Curr. Opin. Infect. Dis.*, **22**, 167 (2009).
[4]   Tuberculosis 2013 European League Foundation. (2013). https://www.europeanlung.org/ en/lung-disease-and-information/lung-diseases/tuberculosis.
[5]   M. Alemayehu, B. Gelaw, E. Abate, L. Wassie, Y. Belyhun, S. Bekele, R.R. Kempker, H.M. Blumberg, A. Aseffa. *Int. J. Mycobacteriol.*, **3**, 132 (2014).
[6]   Z.F. Udwadia, R.A. Amale, K.K. Ajbani, C. Rodrigues. *Clin. Infect. Dis.*, **54**, 579 (2012).
[7]   B. Müller, S. Borrell, G. Rose, S. Gagneux. *Trends Genet.*, **29**, 160 (2013).
[8]   N. Fogel. *Tuberculosis (Edinb)*, **95**, 527 (2015).
[9]   J. Rylance, M. Pai, C. Lienhardt, P. Garner. *Lancet. Infect. Dis.*, **10**, 886 (2010).
[10]  M. Altaf, H. Stoeckli-Evans, A. Cuin, D.N. Sato, F.R. Pavan, C.Q.F. Leite, S. Ahmad, M. Bouakka, M. Mimouni, F.Z. Khardli, T.B. Hadda. *Polyhedron*, **62**, 138 (2013).

[11]  Y.K. Abhale, A. Shinde, K.K. Deshmukh, L. Nawale, D. Sarkar, P.C. Mhaske. *Med. Chem. Res.* , **26**, 2557 (2017).

[12]  R.A. Rane, S.S. Naphade, P.K. Bangalore, M.B. Palkar, M.S. Shaikh, R. Karpoormath. *Bioorg. Med. Chem. Lett.*, **24**, 3079 (2014).

[13]  L.G. Dover, A. Alahari, P. Gratraud, J.M. Gomes, V. Bhowruth, R.C. Reynolds, G.S. Besra, L. Kremer. *Antimicrob. Agents Chemother.*, **51**, 1055 (2007).

[14]  J. Joseph, K. Nagashri, G.B. Janaki. *Eur. J. Med. Chem.*, **49**, 151 (2012).

[15]  D. Banerjee, P. Yogeeswari, P. Bhat, A. Thomas, M. Srividya, D. Sriram. *Eur. J. Med. Chem.*, **46**, 106 (2011).

[16]  B. Demoro, R.F.M. de Almeida, F. Marques, C.P. Matos, L. Otero, J. Costa Pessoa, I. Santos, A. Rodríguez, V. Moreno, J. Lorenzo, D. Gambino, A.I. Tomaz. *Dalton Trans.*, **42**, 7131 (2013).

[17]  D.L. Klayman, J.F. Bartosevich, T.S. Griffin, C.J. Mason, J.P. Scovill. *J. Med. Chem.*, **22**, 855 (1979).

[18]  A. Siwek, J. Stefańska, K. Dzitko, A. Ruszczak. *J. Mol. Model.*, **18**, 4159 (2012).

[19]  K.D. Thomas, A.V. Adhikari, I.H. Chowdhury, T. Sandeep, R. Mahmood, B. Bhattacharya, E. Sumesh. *Eur. J. Med. Chem.*, **46**, 4834 (2011).

[20]  M.V.N. de Souza, K.C. Pais, C.R. Kaiser, M.A. Peralta, M. de, L. Ferreira, M.C.S. Lourenço. *Bioorg. Med. Chem.*, **17**, 1474 (2009).

[21]  F. Conradie, A.H. Diacon, N. Ngubane, P. Howell, D. Everitt, A.M. Crook, C.M. Mendel, E. Egizi, J. Moreira, J. Timm, T.D. McHugh, G.H. Wills, A. Bateson, R. Hunt, C. Van Niekerk, M. Li, M. Olugbosi, M. Spigelman, Nix-TB Trial Team. *NJ. Med. Engl. J. Med.*, **382**, 893(2020).

[22]  C.E. Barry. *N. Engl. J. Med.*, **360**, 2466 (2009).

[23]  O. Afzal, S. Kumar, M.R. Haider, M.R. Ali, R. Kumar, M. Jaggi, S. Bawa. *Eur. J. Med. Chem.*, **97**, 871 (2015).

[24]  M. Foley, L. Tilley. *Pharmacol. Ther.*, **79**, 55 (1998).

[25]  R. Sharma, P. Kour, A. Kumar. *J. Chem. Sci.*, **130**, 73 (2018).

[26]  M. Ratheesh, G. Sindhu, A. Helen. *Inflamm. Res.*, **62**, 367 (2013).

[27]  Z.-C. Liu, B.-D. Wang, Z.-Y. Yang, Y. Li, D.-D. Qin, T.-R. Li. *Eur. J. Med. Chem.*, **44**, 4477 (2009).

[28]  S. Adsule, V. Barve, D. Chen, F. Ahmed, Q.P. Dou, S. Padhye, F.H. Sarkar. *J. Med. Chem.*, **49**, 7242 (2006).

[29]  A.D. Naik, S.M. Annigeri, U.B. Gangadharmath, V.K. Revankar, V.B. Mahale. *J. Mol. Struct.*, **616**, 119 (2002).

[30]  O.V. Dolomanov, L.J. Bourhis, R.J. Gildea, J.A.K. Howard, H. Puschmann. *J. Appl. Crystallogr.*, **42**, 339 (2009).

[31]  G. Sheldrick. *Acta Crystallogr. Sect. A Found Adv.*, **71**, 3 (2015).

[32]  A. Spek. *J. Appl. Crystallogr.*, **36**, 7 (2003).

[33]  MVNdS.; Maria, C.S.; Lourenço, A.C.; Pinheiro, M. d L.; Ferreira, R.S.B.; Gonçalves, T.C.M.; Nogueira, M.A.; Peraltab. ARKIVOC, xv 11 (2007).

[34]  M.R. Peram, S. Jalalpure, V. Kumbar, S. Patil, S. Joshi, K. Bhat, P. Diwan. *J. Liposome Res.*, **29**, 291 (2019).

[35]  A. Castineiras, D.X. West, H. Gebremedhin, T.J. Romack. *Inorg. Chim. Acta*, **216**, 229 (1994).

[36]  V. Kamat, A. Kotian, A. Nevrekar, K. Naik, D. Kokare, V.K. Revankar. *Inorg. Chim. Acta*, **466**, 625 (2017).

[37]  G.A. Gamov, M.N. Zavalishin, A.Y. Khokhlova, A.V. Gashnikova, V.V. Aleksandriiskii, V.A. Sharnin. *J. Coord. Chem.*, **71**, 3304 (2018).

[38]  J.L. Hickey, P.J. Crouch, S. Mey, A. Caragounis, J.M. White, A.R. White, P.S. Donnelly. *Dalton Trans.*, **40**, 1338 (2011).

[39]  A. Kotian, K. Kumara, V. Kamat, K. Naik, D.G. Kokare, A. Nevrekar, N.K. Lokanath, V.K. Revankar. *J. Mol. Struct.*, **1156**, 115 (2018).

[40]  W.J. Geary. *Coord. Chem. Rev.*, **7**, 81 (1971).

[41]  P.P. Netalkar, S.P. Netalkar, S. Budagumpi, V.K. Revankar. *Eur. J. Med. Chem.*, **79**, 47 (2014).

[42] M.A. Ali, SMM-u-H. Majumder, R.J. Butcher, J.P. Jasinski, J.M. Jasinski. *Polyhedron*, **16**, 2749 (1997).

[43] A. Basu, D. Thiyagarajan, C. Kar, A. Ramesh, G. Das. *RSC Adv*, **3**, 14088 (2013).

[44] D.X. West, A.A. Nassar, F.A. El-Saied, M.I. Ayad. *M.I. Ayad. Transit. Met. Chem.*, **24**, 617 (1999).

[45] A.B.P. Lever. *Inorganic Electronic Spectroscopy*, 2nd edn., Elsevier, Amsterdam (1984).

[46] D.X. West, J.K. Swearingen, J. Valdés-Martıńez, S. Hernández-Ortega, A.K. El-Sawaf, F. van Meurs, A. Castiñeiras, I. Garcia, E. Bermejo. *Polyhedron*, **18**, 2919 (1999).

[47] S.S. Bhat, A.A. Kumbhar, H. Heptullah, A.A. Khan, V.V. Gobre, S.P. Gejji, V.G. Puranik. *Inorg. Chem.*, **50**, 545 (2011).

[48] N. Raman, J. Dhaveethu Raja, A. Sakthivel. *J. Chem. Sci.*, **119**, 303 (2007).

[49] G.S. Hegde, S.P. Netalkar, V.K. Revankar. *Appl. Organomet. Chem.*, **33**, e4840 (2019).

[50] D. Kivelson, R. Neiman. *J. Chem. Phys.*, **35**, 149 (1961).

[51] S. Srinivasan, P. Athappan, G. Rajagopal. *Transit. Met. Chem.*, **26**, 588 (2001).

[52] B. Tweedy. *Phytopathology*, **55**, 910 (1964).

[53] N. Dharmaraj, P. Viswanathamurthi, K. Natarajan. *Transit. Met. Chem.*, **26**, 105 (2001).

[54] J.C. Pritchett, L. Naesens, J. Montoya. Chapter 19 - Treating HHV-6 infections: the laboratory efficacy and clinical use of anti-HHV-6 agents, in: L. Flamand, I. Lautenschlager, G.R.F. Krueger, D.V. Ablashi (Eds.), *Human Herpesviruses HHV-6A, HHV-6B & HHV-7*, 3rd edn, Elsevier, Boston, pp. 311–331 (2014).

[55] A.O. de Souza, R.R. Santos, Jr, D.N. Sato, M.M.M. de Azevedo, D.A. Ferreira, P.S. Melo, M. Haun, C.L. Silva, N. Durán. *J. Braz. Chem. Soc.*, **15**, 682 (2004).